DOI 10.1002/mnfr.201200082 *Mol. Nutr. Food Res.* 2012, *56*, 1464–1476

RESEARCH ARTICLE

HPMC supplementation reduces abdominal fat content, intestinal permeability, inflammation, and insulin resistance in diet-induced obese mice

Hyunsook Kim[1,2], Glenn E. Bartley[2], Scott A. Young[3], Paul A. Davis[1] and Wallace Yokoyama[2]

[1] Department of Nutrition, University of California, Davis, CA, USA
[2] USDA, ARS, Western Regional Research Center, Albany, CA, USA
[3] Dow Wolff Cellulosics, Midland, MI, USA

Received: February 7, 2012
Revised: April 20, 2012
Accepted: May 18, 2012

Scope: The effects of hydroxypropyl methylcellulose (HPMC), a highly viscous nonfermentable soluble dietary fiber, were evaluated on adipose tissue inflammation and insulin resistance in diet-induced obese (DIO) mice fed a high-fat (HF) diet supplemented with either HPMC or insoluble fiber.

Methods and results: DIO C57BL/6J mice were fed a HF diet supplemented with 6% HPMC or 6% microcrystalline cellulose (MCC). Gene expression analyses of epididymal adipose tissue by exon microarray and real-time PCR along with glucose and insulin tolerance and intestinal permeability were assessed. HPMC-fed mice exhibited significantly reduced body weight gain and adipose tissue weight as well as reduced areas under the curve for 2-h insulin and glucose responses. HPMC significantly decreased HF diet-induced intestinal permeability. Overall, HPMC enhanced insulin sensitivity and glucose metabolism and downregulated genes related to inflammation and immune response, adipogenesis, and oxidative stress markers. Pathway analysis of microarray data identified lipid metabolism, inflammatory disease, and acute phase response pathways as being differentially regulated by HPMC.

Conclusion: These results suggest HPMC consumption ameliorates HF diet effects on obesity-induced insulin resistance, adipose tissue inflammatory and immune responses, weight gain, as well as intestinal permeability.

Keywords:
Adipogenesis / Inflammation / Insulin sensitivity / Intestinal permeability / Soluble dietary fiber

1 Introduction

Chronic low-grade systemic inflammation is linked to the onset of insulin resistance (IR) in type 2 diabetes and obesity [1]. Lipopolysaccharides (LPS), the cell wall component of gram-negative bacteria, stimulate pro-inflammatory cytokine production [2] and increased circulating LPS has been observed in type 2 diabetic humans and diet-induced obesity (DIO) and genetically obese mice [3–7]. More directly, infusion of LPS results in metabolic diseases in mice while germ-free mice or mice treated to reduce their gram-negative bacteria load do not exhibit high-fat diet-induced inflammatory abnormalities. Furthermore, circulating LPS levels are affected by altered intestinal permeability to LPS across the epithelial barrier [8]. Studies over the last decade suggest that macrophage infiltration and innate and adaptive immune alterations in adipose tissue play a dynamic and pivotal role in the increased expression and production of pro-inflammatory cytokine such as interleukins (ILs) and TNF-α [9, 10]. Intriguingly, LPS has been shown to bind to toll-like receptor 4 (TLR4) found in insulin-targeted tissues including adipose tissue and involved in the signaling pathway of TNF-α production [11].

Diets rich in dietary fibers including soluble dietary fiber (SDF) have recently attracted great interest as they reduced biomarkers of systemic inflammation and IR along with modulating circulating LPS levels in humans or animals [12–14]. For example, diets enriched in soluble fibers, such as apple

Correspondence: Dr. Hyunsook Kim, Department of Nutrition, University of California, Davis, One Shields Avenue, Davis, CA 95616, USA
E-mail: hyskim@ucdavis.edu
Fax: +1-530-752-8632

Abbreviations: HF, high fat; **HPMC**, hydroxypropyl methylcellulose; **IR**, insulin resistance; **SDF**, soluble dietary fiber; **SFRP5**, secreted frizzled-related sequence protein 5

pectin, β-glucan, soluble cocoa fiber, and husk of plantago ovata, improved biomarkers for inflammation or immune system in Zucker fatty rats [15, 16]. Mice fed soluble fiber (pectin) upregulated IL-4 protein expression in spleen and ileum when treated with intraperitoneal endotoxin [17]. In patients with metabolic syndrome, consumption of a high-fiber oat–wheat–potato diet modulated subcutaneous adipose tissue genes related to oxidative stress, inflammation, and interleukin cytokines [18]. Fermentable soluble fiber intake improved intestinal barrier function and decreased circulating LPS levels in high-fat (HF) DIO mice possibly via increased expression of tight-junction proteins [14, 19].

Hydroxypropyl methylcellulose (HPMC) is a nonfermentable, semisynthetic cellulose derivative with the physiological properties of a SDF; e.g. psyllium and β-glucan. Several animal and human studies have found that consumption of HPMC with increasing solution viscosity was associated with increased fecal excretion of bile acids and cholesterol alongside health beneficial effects: hypocholesterolemic and postprandial hypoglycemic effects, adipocytokine alteration, and body weight reduction [20–23]. In a recent study [24], we found that hamsters fed a HF diet with HPMC not only had improved plasma lipid profiles but this was associated with altered hepatic expression of genes related to bile acid and cholesterol as well as fatty acid metabolism.

In contrast to the documented effects of HPMC in nonobese animals fed a HF diet, little is known about the effects of HPMC supplementation in obese animals and on obesity-related inflammation and insulin resistance. As abdominal adipose tissue is the functionally dominant target site of pro-inflammatory cytokines production, we conducted a gene expression analysis using microarray technology in adipose tissue obtained from HF-induced obese mice fed either 6% HPMC or 6% microcrystalline cellulose (MCC).

2 Materials and methods

2.1 Animals and diets

Male C57BL/6J mice were purchased from Charles River Laboratories (Wilmington, MA, USA). The mice were housed individually in an environmentally controlled room (20–22°C, 60% relative humidity, 12-h alternating light:dark cycle). Mice were acclimatized and given ad libitum access to water and mouse chow diet (LabDiet #5015, PMI International, Redwood, CA, USA) for 1 week prior to the initiation of the experimental diets. Mice were weighed and randomized into two groups of 30 mice each. Mice were fed ad libitum either mouse chow diet or HF diets containing 17% of energy as protein, 37% as carbohydrate, and 47% as fat with 0.1% cholesterol. After 5 weeks, mice were weighed and obese mice were identified as those having gained significantly greater weight compared to the mice fed chow diet. The obese mice were then randomized into two groups ($n = 10$ each) and fed ad libitum for 5 weeks HF diets either containing 6% HPMC (The Dow Chemical Company, Midland, MI, USA) or 6% MCC (Dyets, Bethlehem, PA, USA), an insoluble fiber with little effect on sterol metabolism [25] as a control diet (Table 1). Body weights were recorded weekly and food intake was monitored twice per week. The study protocol, #P-04–02, was approved with permission by the Animal Care and Use Committee, Western Regional Research Center, USDA, Albany, CA, USA.

Table 1. Diet composition

Ingredient/Diet type	6% MCC	6% HPMC
Lard fat	225	225
Soybean oil	25	25
Cholesterol	0.8	0.8
MCC[a)]	60	0
HPMC	0	60
Casein	200	200
Corn Starch	138.2	138.2
Sucrose	300	300
DL Methionine	3	3
Choline Bitartrate	3	3
Mineral mix	35	35
Vitamin mix	10	10
Total diet (g)	1000	1000
Fat percent of total energy	46.8	
Protein percent of total energy	16.7	
Carbohydrate percent of total energy	36.5	

a) MCC (microcrystalline cellulose, control): nonviscous water-insoluble fiber.

2.2 Plasma and adipose tissue collection

Mice were feed deprived for 12 h and anesthetized with Isoflurane (Phoenix Pharmaceutical, St. Joseph, MO, USA). Blood was collected by cardiac puncture with syringes previously rinsed with potassium EDTA solution (15% wt/v). The plasma was separated after centrifugation at 2000 × *g* for 30 min at 4°C. Epididymal and subcutaneous adipose tissues were collected, weighed, and immediately frozen in liquid nitrogen for analysis.

2.3 Plasma glucose and lipids analysis

Blood glucose concentration in feed-deprived mice was measured in tail vein samples using a OneTouch Ultrameter (LifeScan Inc., Milpitas, CA, USA). Plasma lipoprotein cholesterol was determined by size-exclusion chromatography as previously described [26]. Briefly, an Agilent 1100 chromatograph was employed with a postcolumn derivatization reactor, consisting of a mixing coil (#1615–50 Bodman, Aston, PA, USA) in a temperature-controlled water jacket (Aura Industrials, Staten, NY, USA). Fifteen microliters of plasma was injected onto a Superose 6HR HPLC column (Pharmacia LKB Biotechnology, Piscataway, NJ, USA). The

lipoprotein fractions were eluted with a pH 7.0 buffer solution containing 0.15 M NaCl and 0.02% sodium azide at a flow rate of 0.5 mL/min. A Hewlett-Packard (Agilent, Palo Alto, CA, USA) HPLC pump 1050 was used to deliver cholesterol reagent (Roche Diagnostics, Indianapolis, IN, USA) at a flow rate of 0.2 mL/min. Bovine cholesterol lipoprotein standards (Sigma Aldrich, St. Louis, MO, USA) were used to calibrate the signal on the basis of peak areas.

2.4 Glucose tolerance test (GTT) and insulin tolerance test (ITT)

Both tests were done after 5 weeks of diet treatment. After 3 h of fasting, mice were injected intraperitoneally with glucose (2 g/kg body weight) and tail vein blood glucose levels were determined at 0, 15, 30, 60, and 120 min after glucose injection using a OneTouch Ultrameter (LifeScan Inc.). ITT was performed with mice injected intraperitoneally with insulin (0.5 U/kg body weight) after 3 h of fasting. Blood glucose levels were determined from tail vein blood at 0, 30, and 60 min after insulin injection using a OneTouch Ultrameter.

2.5 In vivo intestinal permeability

HPMC and MCC diet effects on intestinal permeability to 4000 Da MW fluorescein isocyanate labeled dextran polymer (FITC-dextran) (Sigma-Aldrich, St. Louis, MO, USA) were measured [19]. After 6 h of fasting, mice were administrated by gavage with FITC-dextran (600 mg/kg body weight, 125 mg/mL). After 1 h, 120 μL of blood was collected from the tail vein and centrifuged at 4°C, 12,000 × *g* for 5 min. Fifty microliter of blood was diluted with equal volume of PBS (pH 7.4) and the blood FITC-dextran concentration was analyzed with a fluorescence spectrophotometer (HTS-7000 plus-plate-reader; Perkin Elmer, Wellesley, MA, USA) at an excitation wavelength of 485 nm and emission wavelength of 535 nm. A standard curve of FITC-dextran diluted in non-treated blood diluted with PBS (1:2 [vol/vol]) was used to determine FITC-dextran concentration.

2.6 Gene expression and exon microarray analysis

Total RNA from epididymal adipose tissues was extracted using TRIzol®plus RNA purification kit (Invitrogen, Life Technologies, Carlsbad, CA, USA) from three biological replicates of epididymal adipose tissues per each treatment. Quality of total RNA was determined using a 2100 Bioanalyzer instrument and RNA 6000 Nano LabChip assay (Agilent Technologies, Palo Alto, CA, USA) and 10 μg of total RNA was then used to synthesize one-cycle cDNA (first-strand and second-strand cDNA synthesis) followed by clean-up of double-stranded cDNA and biotin-labeled cRNA synthesis. The biotin-labeled cRNA was used for fragmentation for target preparation using One-Cycle Target Labeling and Control reagents (Affymetrix, Santa Clara, CA, USA). Fragmented cRNA samples were hybridized to a Affymetrix GeneChip® Mouse exon 1.0 ST Array, an expression and exon splicing array containing 1.2 million probesets representing 80 000 genes. The hybridization signals were acquired and analyzed using the GeneChip Scanner 3000 High-Resolution Scanner (Affymetrix) and the Affymetrix GeneChip Operating Software (GCOS). Analysis of both gene expression and exon alternative splicing from the microarray data was performed using a GeneSpring GX version 11.0 program (Agilent Technologies, Santa Clara, CA, USA). Gene expression was determined to be significant when the fold change value was greater than 1.5. The splice index was defined as the log of the ratio of exon-level expression over gene-level expression. A fold change in splice index value greater than or equal to 2 between treatment and control groups was considered as differentially spliced [27]. Transcripts with at least one differentially spliced exon were considered as differentially regulated splicing [27].

2.7 Real-time RT-PCR

Total RNA from epididymal adipose tissues was extracted using TRIzol®plus RNA purification kit (Invitrogen) and cDNA was synthesized using GeneAmp®RNA PCR kit (Applied Biosystems, Foster City, CA, USA) as per the manufacturer's protocol. One microliter of diluted cDNA (1:10) was used in each real-time RT-PCR using SYBR Green Supermix (Bio-Rad, Hercules, CA, USA) with an Mx3000P instrument (Stratagene, Cedar Creek, TX, USA). The cycle conditions were: 5 min at 95°C followed by 40 cycles of incubation at 94°C for 15 s, then 55–60°C for 1 min and 72°C for 30 s. The sequences of the primers used for this study are shown in supporting information Table 1. The primers were validated by size and sequencing of PCR products. No accumulation of nonspecific products and primer-dimers was observed in a gel electrophoresis test of the PCR products. The results were analyzed using the software provided with the Stratagene Mx3000P QPCR system. Differences in mRNA expression were calculated after normalizing to *36B4* expression.

2.8 Statistical analysis

All data are expressed as means ± SE. Analysis of variance (ANOVA) was performed to examine the effect of treatment on plasma lipid levels, body and tissue weights, and energy intake using the JMP®7 statistical program (SAS Institute, Cary, NC, USA). Significance was defined at $p < 0.05$. Statistical analysis of differences in microarray analysis data using GeneSpring GX 11.0 program was performed by unpaired

student's *t*-test. Ingenuity pathway analysis (IPA, Ingenuity® Systems, Redwood City, CA, USA) was used to identify biological functions, canonical pathway, and network pathway that were most significant to the dataset. Significance was assigned when a p less than 0.05 was calculated using the right-tailed Fisher's exact test. The probability that each biological function for dataset, association between genes in the dataset and the canonical pathway, and biological function and/or disease assigned to that network for that dataset was explained by change alone.

3 Results

3.1 Metabolic effect of HPMC supplementation

The body weight gain and total energy intake were significantly less in the HPMC group compared with the control group, resulting in a 60% lower energy efficiency ratio in the HPMC group (Table 2). Liver, epididymal, and subcutaneous adipose weights of the HPMC group were 13, 49, and 51% lower, respectively, than those of control group ($p < 0.05$) (Table 2). While plasma LDL-cholesterol concentration was 45% lower than that of the control group ($p < 0.05$) (Fig. 1), plasma VLDL-, HDL-, and total-cholesterol concentrations did not differ between the control and HPMC groups (Fig. 1).

3.2 Effect of HPMC supplementation on glucose and insulin response

Dietary HPMC supplementation significantly lowered peak glucose response at 30 min ($p < 0.05$) and area under the curve during a 2-h glucose response (Fig. 2A and B). HPMC supplementation also resulted in a marked reduction of insulin response at 30 min ($p < 0.05$) and 60 min ($p < 0.05$) and area under the curve during a 2-h insulin response (Fig. 3A and B).

Table 2. Anthropometrics and blood glucose concentrations in mice fed 6% MCC or HPMC diet for 5 weeks[a)]

	6% MCC	6% HPMC
Body weight gain (g)	10.3 ± 1.58	4.61 ± 0.55*
Total energy intake (Kcal)	419 ± 9.13	356 ± 9.83*
Liver weight (g)	1.08 ± 0.04	0.94 ± 0.02*
Epididymal adipose tissue weight (g)	1.97 ± 0.14	1.01 ± 0.15*
Subcutaneous adipose tissue weight (g)	1.11 ± 0.11	0.54 ± 0.09*
Blood glucose (mg/dL)	222 ± 18.2	196 ± 12.7

a) Values are means ± SE, $n = 10$.
*Different from MCC, $p < 0.05$.

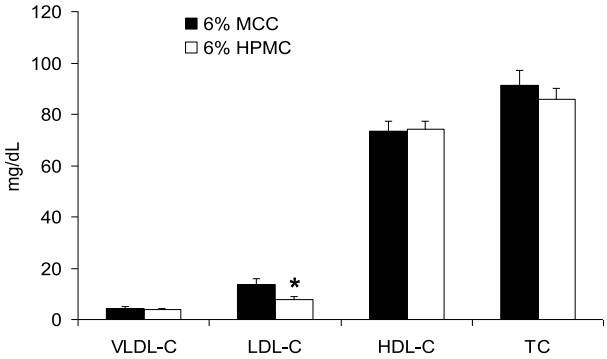

Figure 1. Concentration of plasma lipids in obese mice fed0 HF diet supplemented with either 6% HPMC or 6% MCC for 5 weeks. Blood was collected in fasting state. Data are expressed as mean ± SE. $n = 10$/group. Asterisk (*) indicates significant difference at $p < 0.05$.

3.3 Effect of HPMC supplementation on expression of genes related to inflammation in adipose tissue

The levels of gene expression of CD68, a macrophage marker, and TNF-α, a pro-inflammatory cytokine, were downregulated by 0.4- and 0.6-fold, respectively, in the HPMC group relative to the control group. The relative mRNA levels of leptin and TLR-4 were downregulated by 0.3- and 0.7-fold, respectively, in the HPMC group while adiponectin mRNA was upregulated by 1.3-fold in the HPMC group compared to the control group (Fig. 4).

3.4 Microarray analysis of adipose tissue gene expression profiles

The comprehensive expression of genes in adipose tissue of mice fed HF diets supplemented with either 6% MCC or 6% HPMC was assessed by microarray analysis (Mouse exon 1.0 ST array, Affymetrix). A total of 74 genes including six unnamed genes were differentially expressed in mice fed 6% HPMC compared to 6% MCC ($p < 0.05$, fold change > 1.5) (Supporting information Table 2). Among these genes, 56 were downregulated and 18 upregulated. Table 3 shows the selected genes differentially down- and upregulated genes by HPMC based on biological process of gene ontology descriptions. Molecules involved in response to innate immunity and inflammation, such as annexin A1 (Anxa1l; fold change: –1.9), lipopolysaccharide-binding protein (LBP; fold change: –2.0), major histocompatibility complex, class I related (Mr1; fold change: –1.7), histocompatibility 2 Q region locus 6 (H2-Q6; fold change: –1.7), histone

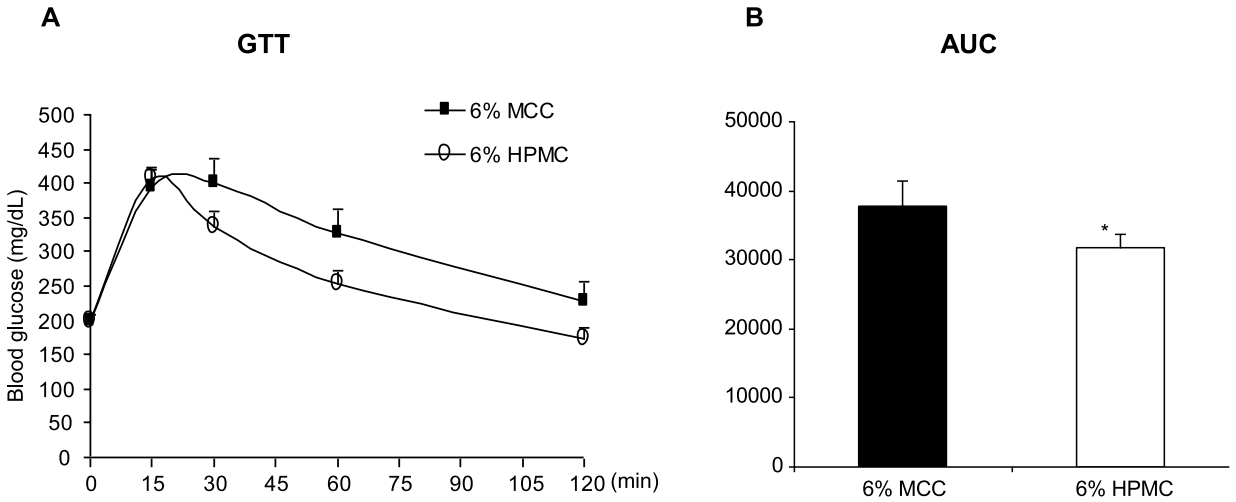

Figure 2. Glucose tolerance in obese mice fed HF diet supplemented with either 6% HPMC or 6% MCC for 5 weeks. (A) Glucose tolerance tests (GTT) were performed in the fasting state. (B) Area under the curve values. Data are expressed as mean ± SE. $n = 8$–9/group. Asterisk (*) indicates significant difference at $p < 0.05$.

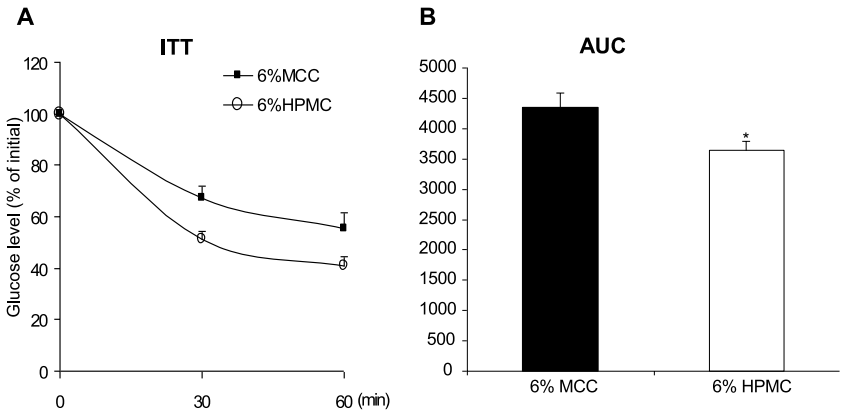

Figure 3. Insulin tolerance in obese mice fed HF diet supplemented with either 6% HPMC or 6% MCC for 5 weeks. (A) Insulin tolerance tests (ITTs) were performed in the fasting state. (B) Area under the curve values. Data are expressed as mean ± SE. $n = 8$–9/group. Asterisk (*) indicates significant difference at $p < 0.05$.

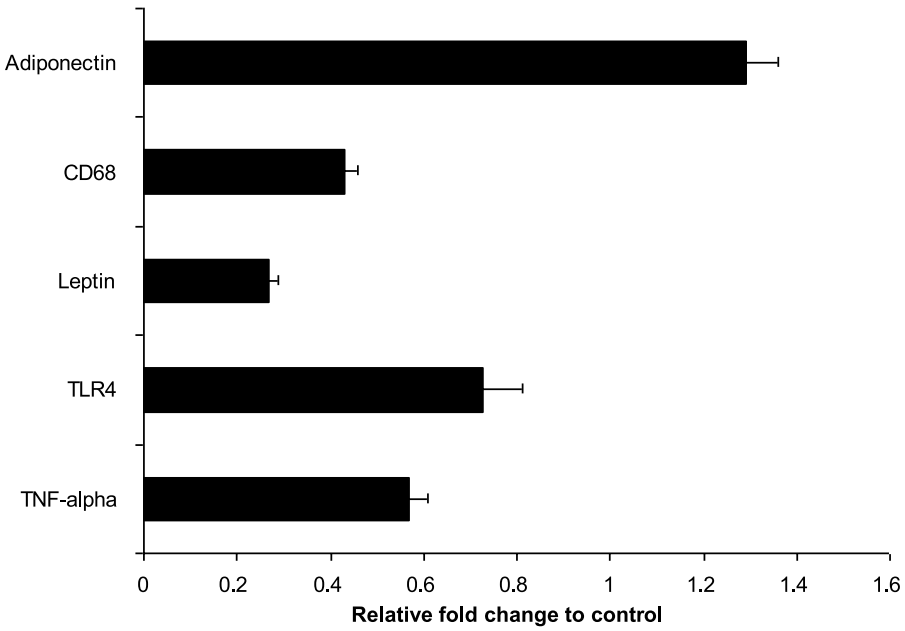

Figure 4. Relative adipose expression of adiponectin, CD68, leptin, TLR4, and TNF-α genes in obese mice fed HF diet supplemented with either 6% HPMC or 6% MCC for 5 weeks. Data are expressed as mean ± SE. $n = 6$/group.

Table 3. Summary of selected genes significantly downregulated or upregulated by HPMC in adipose tissue of mice fed HF diet supplemented with HPMP (fold change $\geq$ 1.5)

Biological process (GO)[a)]	Symbol	Name	Fold change	Gene ID
Downregulated				
α-β T cell differentiation involved in immune response	Anxa1	Annexin A1	–1.9	CT009771
Activation of phospholipase C activity by G-protein coupled receptor protein signaling pathway	Npr3	Natriuretic peptide receptor 3	–1.5	BC055897
Acute phase response, Cellular response to lipopolysaccharide	Lbp	Lipopolysaccharide binding protein	–2.0	BC004795
Age-dependent response to oxidative stress	Sod2	Superoxide dismutase 2, mitochondrial	–1.9	BC010548
Angiogenesis	Fgf1	Fibroblast growth factor 1	–1.6	U67610
	Mmp19	Matrix metallopeptidase 19	–1.7	AF155221
	Fgf13	Fibroblast growth factor 13	–4.6	BC018238
	Tfpi2	Tissue factor pathway inhibitor 2	–1.6	D50586
Antigen processing and presentation	Mr1	Major histocompatibility complex, class I-related	–1.7	BC026137
Antigen processing and presentation of peptide antigen via MHC class I	H2-Q6	Histocompatibility 2 Q region locus 6	–1.7	BC010602
B cell differentiation	Hdac9	Histone deacetylase 9	–1.8	BC098187
Carbohydrate metabolic process	Gpd1	Glycerol-3-phosphate dehydrogenase 1	–2.2	BC019391
Cartilage development	Bmp3	Bone morphogenetic protein 3	–1.7	BC117749
Cell cycle	Ccnd2	Cyclin D2	–1.6	M83749
Cholesterol biosynthetic process	Insig1	Insulin induced gene 1	–2.5	BC132167
Diacylglycerol biosynthetic process	Mogat2	Monoacylglycerol O-acyltransferase 2	–1.6	BC052831
Endocytosis (Macrophage receptor)	Mrc2	Mannose receptor C type 2	–3.2	U56734
Fatty acid biosynthetic metabolic process	Elovl6	ELOVL family member 6 elongation of long chain fatty acids	–1.8	AY053453
Fatty acid biosynthetic process	Scd2	Stearoyl-Coenzyme A desaturase 2	–4.2	BC040384
Lipid biosynthetic process	Dgat2	Diacylglycerol O-acyltransferase 2	–2.1	BC043447
Lipid catabolic process	Pafah2	Platelet-activating factor acetylhydrolase 2	–1.5	BC025495
Lipid catabolic process	Lipf	Lipase gastric	–2.1	BC061067
Lipid metabolic process	Sgms2	Sphingomyelin synthase 2	–1.5	BC117782
Negative regulation of activation of membrane attack complex	(Cd59a|Cd59b)	CD59a antigen | CD59b antigen	–1.6	U60473
Oxidation–reduction process	Pam	Peptidylglycine alpha-amidating monooxygenase	–2.0	U79523
Phospholipids biosynthetic process	Lpgat1	Lysophosphatidylglycerol acyltransferase 1	–2.3	AK172914
Unknown	Gpc4	Glypican 4	–1.7	BC006622
Wnt receptor signaling pathway	Sfrp5	Secreted frizzled-related sequence protein 5	–2.6	BC032921
Upregulated				
Acute inflammatory response (antiapoptosis)	Vnn1	Vanin 1	2.5	BC019203
Circadian regulation of gene expression	Rbm4	RNA-binding motif protein 4	1.5	BC130256
Muscle organ development	Tagln	Transgelin	1.5	L41154

a) Genes were classified into categories depending on the putative biological process in which they are involved according to the classification used by the Gene Ontology Consortium (GO).

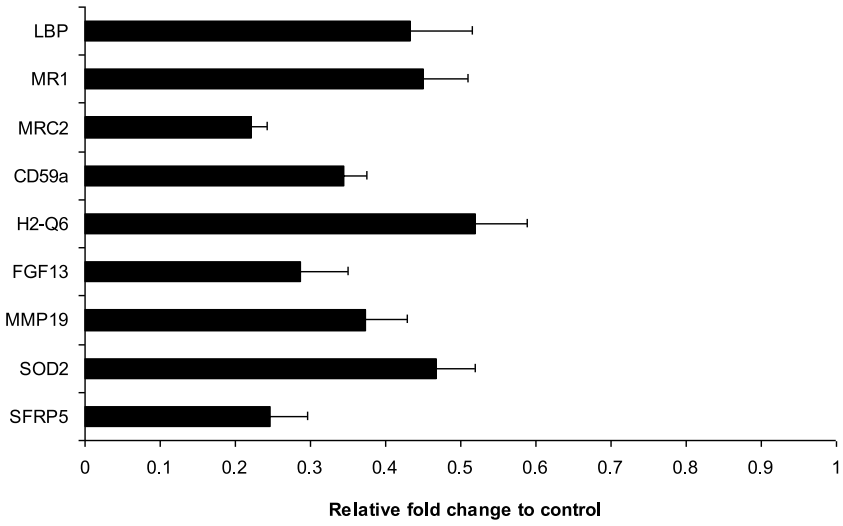

Figure 5. Relative adipose expression of LBP, MR1, MRC2, CD59a, H2-Q6, FGF13, MMP19, SOD2, and SFRP5 genes in obese mice fed HF diet supplemented with either 6% HPMC or 6% MCC for 5 weeks. Data are expressed as mean ± SE. $n = 5$/group.

deacetylase 9 (Hdac9; fold change: –1.8), mannose receptor C type 2 (Mrc2; fold change: –3.2), and CD59a antigen (CD59a; fold change: –1.6), were downregulated in mice fed HPMC compared to the MCC. Genes involved in lipid biosynthetic processes were also downregulated, including monoacylglycerol O-acyltransferase 2 (Mogat2; fold change: –1.6), ELOVL family member 6 elongation of long chain fatty acids (Elovl6; fold change: –1.8), stearoyl-coenzyme A desaturase 2 (Scd2; fold change: –4.2), diacylglycerol O-acyltransferase 2 (Dgat2; fold change: –2.1), platelet-activating factor acetylhydrolase 2 (Pafah2; fold change: –1.5), lipase gastric (Lipf; fold change: –2.1), sphingomyelin synthase 2 (Sgms2; fold change: –1.5), and lysophosphatidylglycerol acyltransferase1 (Lpgat1; fold change: –2.3). Genes involved in angiogenesis, such as fibroblast growth factor 1 (Fgf1; fold change: –1.6), matrix metallopeptidase 19 (Mmp19; fold change: –1.7), fibroblast growth factor 13 (Fgf13; fold change: –4.6), tissue factor pathway inhibitor 2 (Tfpi2; fold change: –1.6), were downregulated following HPMC supplementation. Superoxide dismutase 2 (Sod2; fold change: –1.9), which is related to oxidative stress metabolism, was also downregulated. On the other hand, vanin 1 (Vnn1; fold change: +2.5), which is involved in antiapoptosis and inflammatory response, was upregulated following HPMC supplementation. The observed microarray results were confirmed by RT-PCR analysis. Expression of genes related to innate immune and inflammatory response, including LBP, MR1, MRC2, CD59a, and H2-Q6 was downregulated in the HPMC group compared to the control group (Fig. 5). The expression levels of FGF13 and MMP 19 encoding genes related to angiogenesis were also downregulated by HPMC supplementation (Fig. 5). The mRNA level of SOD2, encoding a gene related to oxidative stress metabolism, was lowered after HPMC supplementation (Fig. 5). Expression of secreted frizzled-related sequence protein 5 (SFRP5), recently identified as an obesity gene, was downregulated following HPMC treatment (Fig. 5).

To explore further the role of differentially expressed genes by HPMC supplementation, we conducted a pathway analysis using IPA System and identified several biological functions and canonical gene pathways differentially regulated by HPMC (Table 4). Genes related to biological functions of lipid metabolism were significantly differently expressed. Canonical pathways of glycerolipid and histidine metabolism, LXR/RXR activation, and acute phase response signaling were affected by the HPMC supplementation. In addition, the networks involving lipid metabolism and immunological diseases as well as those involving sterol regulatory element binding transcription factor 1 (SREBF1), a transcription factor that regulates lipid homeostasis, were affected (data not shown).

Analysis of exon data from the microarray using a GeneSpring GX 11.0 program resulted in the identification of only two genes with greater than 1.0 of splicing index (SI) regulated by HPMC supplementation (Mrc 2 = −1.2, LBP = −1.1, $p < 0.05$). However, there were no transcripts with SI greater or equal to 2 (data not shown).

3.5 Effect of HPMC supplementation on intestinal permeability

To investigate whether HPMC supplementation alters HF-induced intestinal permeability, in vivo intestinal permeability was determined by using dextran-4000-FITC after HPMC feeding. Intestinal permeability was 48% lower in the HPMC group than in the control group ($p < 0.05$) (Fig. 6).

4 Discussion

Lipid metabolism, inflammatory and immune response, and angiogenesis were significantly influenced by dietary

Table 4. Top 12 biological functions, top 12 canonical pathways, and top ten network pathways of adipocyte genes that were significantly upregulated or downregulated by HPMC

Biological functions	*p*-value	No. of genes differentially expressed
Lipid metabolism	2.55×10^{-12}–4.52×10^{-03}	67
Molecular transport	2.55×10^{-12}–4.57×10^{-03}	53
Small molecule biochemistry	2.55×10^{-12}–4.57×10^{-03}	78
Renal and urological disease	4.19×10^{-10}–2.56×10^{-03}	38
Nutritional disease	1.31×10^{-09}–3.12×10^{-03}	35
Dermatological diseases and conditions	3.09×10^{-09}–1.1×10^{-03}	59
Genetic disorder	5.61×10^{-09}–4.06×10^{-03}	183
Gastrointestinal disease	1.71×10^{-08}–4.34×10^{-03}	111
Hepatic system disease	1.71×10^{-08}–1.91×10^{-03}	39
Cancer	4.43×10^{-07}–4.34×10^{-03}	107
Endocrine system disorders	4.87×10^{-07}–3.75×10^{-03}	32
Metabolic disease	4.87×10^{-07}–4.45×10^{-03}	83
Inflammatory disease	8.78×10^{-07}–3.57×10^{-03}	101
Ingenuity canonical pathways	*p*-value	Ratio[a)]
Glycerolipid metabolism	1.74×10^{-03}	7/148 (0.047)
Histidine metabolism	1.83×10^{-03}	5/115 (0.043)
LXR/RXR activation	2.46×10^{-03}	6/93 (0.065)
Acute phase response signaling	3.31×10^{-03}	9/178 (0.051)
Glutathione metabolism	3.85×10^{-03}	5/90 (0.056)
Phenylalanine metabolism	5.13×10^{-03}	4/111 (0.036)
Clathrin-mediated endocytosis signaling	8.51×10^{-03}	8/172 (0.047)
MSP-RON signaling pathway	9.33×10^{-03}	4/51 (0.078)
Caveolar-mediated endocytosis signaling	1.07×10^{-02}	5/85 (0.059)
Fatty acid biosynthesis	1.32×10^{-02}	2/49 (0.041)
Citrate cycle	1.48×10^{-02}	3/57 (0.053)
Propanoate metabolism	1.95×10^{-02}	4/121 (0.031)
Network pathways	Score[b)]	Focus molecules[c)]
Lipid Metabolism, small molecule biochemistry, vitamin and mineral metabolism	46	27
Post-translational modification, cell-to-cell signaling and interaction, cellular movement	32	21
Cell cycle, immunological disease, hematological system development and function	32	21
Neurological disease, carbohydrate metabolism, lipid metabolism	31	21
Behavior, tissue morphology, cancer	29	20
Drug metabolism, nucleic acid metabolism, small molecule biochemistry	28	19
Cardiovascular disease, tissue morphology, lipid metabolism	26	18
Lipid metabolism, molecular transport, small molecule biochemistry	24	17
Genetic disorder, skeletal and muscular disorders, cell-to-cell signaling and interaction	23	19
Lipid metabolism, molecular transport, small molecule biochemistry	21	16
Cellular development, cell morphology, cellular compromise	21	16

The functions, canonical, and network pathways that were most significant to the dataset were identified by Ingenuity Pathway Analysis (Ingenuity Systems).
a) Number of molecules (genes) that meet cutoff criteria, divided by total number of molecules that made up in a given pathway.
b) Likelihood of finding the focus molecules in a given pathway, expressed as the negative log of *p*-value.
c) Gene objects that meet cutoff criteria, mapped to other molecules in the Ingenuity Pathways Knowledge Base.

HPMC supplementation of a HF diet in obese mice. HPMC markedly downregulated the expression of selected genes in the adipocyte related to oxidative stress marker (SOD2), angiogenesis (FGF13 and MMP19), acute phase, immune, and inflammatory response (LBP, MR1, MRC2, CD59, H2-Q6). The alterations found in the adipose tissue gene profiles were accompanied by reduced adiposity and energy intake, 50% and 15%, respectively, as compared to the control group.

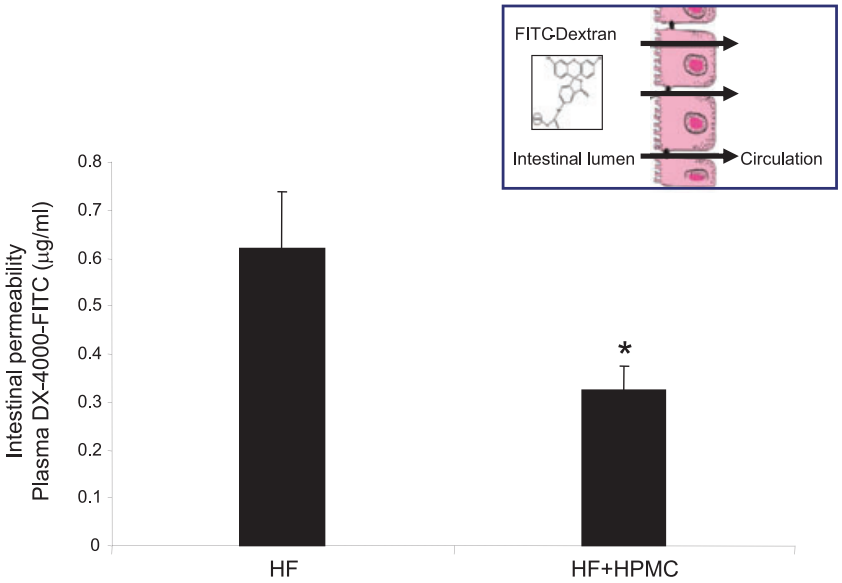

Figure 6. Intestinal permeability measurement by FITC-Dextran gavage and measurement of fluorescence in blood from obese mice fed HF diet supplemented with either 6% HPMC or 6% MCC for 5 weeks. Data are expressed as mean ± SE. $n = 8$–9/group. Asterisk (*) indicates significant difference at $p < 0.05$.

Consistent with our results, previous studies have shown that weight loss suppresses expression of adipose tissue genes related to inflammation in mice and obese subjects [28, 29]. Of note, HPMC supplementation lowered the expression of genes in adipose tissue that are candidate genes in obesity as previously reported such as FGF13, Npr3 [30], BMP3, and Sfrp5 [31].

A significant observation in this study is that expression of LBP, the gene involved in cellular response to LPS was significantly downregulated in adipose tissue from the obese mice fed HPMC. LBP via formation of complexes with LPS functions to present LPS to membrane CD14 in LPS-responsive cells including monocytes and macrophages [32, 33]. While the majority of LBP is produced by the liver, extrahepatic expression of LBP has been reported during acute phase responses [34] and LBP–LPS monomers upregulate TNF-α production in macrophage aggregates around dead adipocytes [35]. In addition, the expression of TLR-4 was downregulated by HPMC supplementation. The TLR-4 gene is activated by gut-mediated LPS binding [36] and is involved in the signaling pathway of TNF-α production [11]. According to recent studies [2, 14, 19], increased circulating LPS is involved in the pro-inflammatory processes. Besides reducing the expression of adipose genes related to pro-inflammatory processes, HPMC supplementation significantly reduced HF diet-induced in vivo intestinal permeability by approximately 50% compared to control diet. Therefore, our results suggest that HPMC and other viscous SDFs by improving intestinal barrier function may have reduced circulating LPS thereby preventing LPS-mediated pro-inflammatory process. We cannot, however, exclude the alternative mechanisms by which other endogenous ligands such as saturated fatty acids [37] and high mobility group box 1 (HMGB1) [38, 39] that directly regulate TLR-4 expression and circulating LPS concentration.

Circulating LPS has also been shown to affect lipoprotein profiles by lowering total and HDL cholesterol in periodontitis patients and animals [40, 41]. On the basis of LBPs significant structural homology with phospholipid transport proteins, e.g. cholesteryl ester transfer protein (CETP) and phospholipid transfer protein (PLTP), LBP mediates the interaction of LPS with lipoproteins. LPS–LBP monomers bind to HDL-cholesterol in healthy plasma while they bind to VLDL–IDL during infection [40, 42]. The increased integrity of intestinal barrier upon HPMC supplementation as measured by FITC-dextran permeability suggests that gastrointestinal LPS absorption was lower in those mice. A lower LPS load in those HPMC supplemented mice may account for the fact that in contrast to other human and animal studies [40, 41], the current study's HDL and VLDL cholesterol were unchanged while LDL cholesterol was significantly lower. This might also be due to different cholesterol metabolism among animal species; in mice, LPS is mostly bound to PLTP perhaps because PLTP is a major protein facilitating transfer of VLDL phospholipids to HDL [43].

With respect to intestinal barrier function, diet could be a modulator via modifying intestinal tight junction integrity through altered protein expression. HF diet-induced intestinal permeability has been shown to be a result of reduced tight junction protein expression in rats [44]. However, diet-related modulation of intestinal microbiota composition may also have an effect as diets with fermentable soluble fiber modifies intestinal microbiota composition and end products of microbial fermentation (short chain fatty acids, SFAs, especially butyrate), and increase expression of tight-junction proteins (ZO-1 and occludin) as well as production of GLP-2 [14]. GLP-2 released from intestinal L-cells, is known as a mediator of improvement of the intestinal barrier function [14]. In addition, bile acids downregulate tight junction protein expression and intestinal permeability to LPS [44, 45] while bile

acid binding resins such as cholestyramine reduce intestinal permeability [46]. Thus, the increased excretion of bile acid found in response to HPMC [20] may have contributed to the improvement of the intestinal barrier function seen in the HPMC supplemented animals. Further studies are required to elucidate the mechanism for HPMC-induced changes in the intestinal permeability.

Adipogenesis is associated with both proliferation and differentiation of preadipocytes during which the expression of subsets of genes encoding mitogenic and adipogenic action is upregulated. In this study, HPMC supplementation significantly downregulated adipose tissue genes that are related to mitogenic action such as Ccnd2, FGF-1 [47], and PAM [48], and genes related to adipocyte differentiation including HDAC9 [49], GPD1 [50], and GPC4 [51]. Interestingly, expression of Tagln [52], also known as smooth muscle actin 22α (SM22α) and the markers of smooth muscle differentiation, was significantly upregulated by HPMC in adipose tissue. Taken together, HPMC supplementation appears to reduce adipogenesis by modulating adipocyte proliferation and differentiation.

Adipose tissue angiogenesis is required for adipocyte differentiation and growth [53]. HPMC supplementation significantly downregulated angiogenic genes such as MMP19 [54], FGF-1 [55], FGF13, TFPI2 [56], SCD2 [57], and ANXA1 [58]. Angiogenesis has been shown to be related to obesity, inflammation, and insulin sensitivity [59–62], and antiangiogenic agents have been reported to increase insulin sensitivity [60]. The downregulation of angiogenic genes found in the HPMC-fed mice suggests that HPMC-induced change in angiogenesis may be an additional explanation for improvement of adiposity, inflammation, and insulin sensitivity found.

Alternative splicing regulation has been associated with obesity and type 2 diabetes. The spliced isoform ratio (Lamin A/C) of Lamin, an extracelluar matrix regulator, was decreased in obese and in type 2 diabetes patients [63]. Moreover, a recent study [64] demonstrated that the splicing factor SFRS10 is downregulated in both the liver and muscle of obese subjects, which increased expression of lipogenic genes. The resulting downregulation in SFRS10 modulated splice isoform of LPIN1, a key regulator of lipid metabolism, by inclusion of exon 6. Dietary status can also regulate alternative splicing variants. HF diet or polyunsaturated fatty acid (PUFA) modulated pre-mRNA splicing of glucose-6-phosphate dehydrogenase (G6PD) [65]. Curcumin, epigallocatechin galate (EGCG), and resveratrol corrected aberrant alternative splicing of survival motor neuron-2 (SMN2) mRNA by increased inclusion of exon 7 in spinal muscular atrophy (SMA) patient [66]. Food restriction induced alternative splicing of resistin mRNA in epididymal adipose tissue of Wistar rats [67]. Dietary HPMC supplementation did not alter the expression of splicing variants of adipocyte genes as exon-array data analysis identified no genes regulated by HPMC feeding with an SI greater or equal to 2. In a separate experiment, transcripts with $|SI| < 2.0$ did not show alternative spliced isoforms evaluated by RT-PCR analysis (data not shown). Curiously, HPMC supplementation did significantly upregulate expression of RNA-binding motif protein (RBM4) gene related to alternative splicing machinery during myogenesis [68].

Impaired glucose tolerance and fasting hyperglycemia both contribute to the development of type 2 diabetes from prediabetic status [69]. Our study revealed that HPMC supplementation significantly improved insulin sensitivity and glucose metabolism as shown by 16% lower AUC during 2 h ITT and GTT compared to the control group. However, HPMC supplementation only tended to lower fasting glucose concentration compared to the control group and did not reach statistical significance. Possibly, fasting glucose concentration after HPMC supplementation may have been lowered by increasing the amount in the diet or longer feeding period.

In summary, we have demonstrated that obese mice fed 6% HPMC in a HF diet had reduced body weight gain and abdominal adipose tissue mass, improved insulin sensitivity, and markedly enhanced glucose tolerance. While antiobesity effect of HPMC supplementation could be mediated by both reduction of energy intake and increases in fecal lipid excretion, HPMC also altered intestinal barrier function. In aggregate, HPMCs effects appear to involve a decreased low-grade inflammatory response via the modulation of genes related to macrophage infiltration, immune response, inflammation, oxidative stress, and adipogenesis in adipose tissue. However, it was not related to changes of alternative splicing regulation. These findings suggest that consumption of a viscous and nonfermentable SDF, HPMC, by reducing obesity-related chronic inflammation and IR in response to a HF meal, may be potentially useful in the prevention of metabolic diseases.

We thank Dr. Michael George, University of California, Davis, for reviewing and editing of methods and Mr. Wanless Hatcher and Mr. Ezekial Martinez for their diligent attention to animal care.

The authors have declared no conflict of interest.

5 References

[1] Pickup, J. C., Inflammation and activated innate immunity in the pathogenesis of type 2 diabetes. *Diabetes Care* 2004, *27*, 813–823.

[2] Brown, J., Wang, H., Hajishengallis, G. N., Martin, M., TLR-signaling networks: an integration of adaptor molecules, kinases, and cross-talk. *J. Dent. Res.* 2011, *90*, 417–427.

[3] Creely, S. J., McTernan, P. G., Kusminski, C. M., Fisher, M. et al., Lipopolysaccharide activates an innate immune system response in human adipose tissue in obesity and type 2 diabetes. *Am. J. Physiol. Endocrinol. Metab.* 2007, *292*, E740–E747.

[4] Nakarai, H., Yamashita, A., Nagayasu, S., Iwashita, M. et al., Adipocyte-macrophage interaction may mediate

LPS-induced low-grade inflammation: potential link with metabolic complications. *Innate Immun.* 2012, *18*, 164–170.

[5] Brun, P., Castagliuolo, I., Di Leo, V., Buda, A. et al., Increased intestinal permeability in obese mice: new evidence in the pathogenesis of nonalcoholic steatohepatitis. *Am. J. Physiol. Gastrointest. Liver Physiol.* 2007, *292*, G518–G525.

[6] Neal, M. D., Leaphart, C., Levy, R., Prince, J. et al., Enterocyte TLR4 mediates phagocytosis and translocation of bacteria across the intestinal barrier. *J. Immunol.* 2006, *176*, 3070–3079.

[7] Dasu, M. R., Devaraj, S., Park, S., Jialal, I., Increased toll-like receptor (TLR) activation and TLR ligands in recently diagnosed type 2 diabetic subjects. *Diabetes Care* 2010, *33*, 861–868.

[8] Suzuki, T., Hara, H., Role of flavonoids in intestinal tight junction regulation. *J. Nutr. Biochem.* 2011, *22*, 401–408.

[9] Xu, H., Barnes, G. T., Yang, Q., Tan, G. et al., Chronic inflammation in fat plays a crucial role in the development of obesity-related insulin resistance. *J. Clin. Invest.* 2003, *112*, 1821–1830.

[10] Chawla, A., Nguyen, K. D., Goh, Y. P., Macrophage-mediated inflammation in metabolic disease. *Nat. Rev. Immunol.* 2011, *11*, 738–749.

[11] Hoareau, L., Bencharif, K., Rondeau, P., Murumalla, R. et al., Signaling pathways involved in LPS induced TNFalpha production in human adipocytes. *J. Inflamm. (Lond).* 2010, *7*, 1.

[12] Qi L, van Dam, R. M., Liu, S., Franz, M. et al., Whole-grain, bran, and cereal fiber intakes and markers of systemic inflammation in diabetic women. *Diabetes Care* 2006, *29*, 207–211.

[13] Ma, Y., Hebert, J. R., Li, W., Bertone-Johnson, E. R. et al., Association between dietary fiber and markers of systemic inflammation in the Women's Health Initiative Observational Study. *Nutrition* 2008, *24*, 941–949.

[14] Cani, P. D., Possemiers, S., Van de Wiele, T., Guiot, Y. et al., Changes in gut microbiota control inflammation in obese mice through a mechanism involving GLP-2-driven improvement of gut permeability. *Gut* 2009, *58*, 1091–1103.

[15] Sanchez, D., Quinones, M., Moulay, L., Muguerza, B. et al., Soluble fiber-enriched diets improve inflammation and oxidative stress biomarkers in Zucker fatty rats. *Pharmacol. Res.* 2011, *64*, 31–35.

[16] Milagros, G., Manuel, S., Rocío, V., Mercedes, G., Anna, A. et al. A diet supplemented with husks of Plantago ovata reduces the development of endothelial dysfunction, hypertension, and obesity by affecting adiponectin and TNF-α in obese Zucker rats. *J. Nutr.* 2005, *135*, 2399–2404.

[17] Sherry, C. L., Kim, S. S., Dilger, R. N., Bauer, L. L. et al., Sickness behavior induced by endotoxin can be mitigated by the dietary soluble fiber, pectin, through up-regulation of IL-4 and Th2 polarization. *Brain Behav. Immun.* 2010, *24*, 631–640.

[18] Kallio, P., Kolehmainen, M., Laaksonen, D. E., Kekalainen, J. et al., Dietary carbohydrate modification induces alterations in gene expression in abdominal subcutaneous adipose tissue in persons with the metabolic syndrome: the FUNGENUT Study. *Am. J. Clin. Nutr.* 2007, *85*, 1417–1427.

[19] Cani, P. D., Bibiloni, R., Knauf, C., Waget, A. et al., Changes in gut microbiota control metabolic endotoxemia-induced inflammation in high-fat diet-induced obesity and diabetes in mice. *Diabetes* 2008, *57*, 1470–1481.

[20] Maki, K. C., Carson, M. L., Kerr Anderson, W. H., Geohas, J. et al., Lipid-altering effects of different formulations of hydroxypropylmethylcellulose. *J. Clin. Lipidol.* 2009, *3*, 159–166.

[21] Maki, K. C., Davidson, M. H., Torri, S., Ingram, K. A. et al., High-molecular-weight hydroxypropylmethylcellulose taken with or between meals is hypocholesterolemic in adult men. *J. Nutr.* 2000, *130*, 1705–1710.

[22] Hung, S. C., Bartley, G., Young, S. A., Albers, D. R. et al., Dietary fiber improves lipid homeostasis and modulates adipocytokines in hamsters. *J. Diabetes* 2009, *1*, 194–206.

[23] Hung, S. C., Anderson, W. H., Albers, D. R., Langhorst, M. L. et al., Effect of hydroxypropyl methylcellulose on obesity and glucose metabolism in a diet-induced obesity mouse model. *J. Diabetes* 2011, *3*, 158–167.

[24] Kim, H., Bartley, G. E., Rimando, A. M., Yokoyama, W., Hepatic gene expression related to lower plasma cholesterol in hamsters fed high-fat diets supplemented with blueberry peels and peel extract. *J. Agric. Food Chem.* 2010, *58*, 3984–3991.

[25] Horton, J. D., Cuthbert, J. A., Spady, D. K., Regulation of hepatic 7 alpha-hydroxylase expression by dietary psyllium in the hamster. *J. Clin. Invest.* 1994, *93*, 2084–2092.

[26] German, J. B., Xu, R., Walzem, R., Kinsella, J.E. et al., Effect of dietary fats and barley fiber on total cholesterol and lipoprotein cholesterol distribution in plasma of hamsters. *Nutr. Res.* 1996, *16*, 1239–1249.

[27] Ortis, F., Naamane, N., Flamez, D., Ladriere, L. et al., Cytokines interleukin-1beta and tumor necrosis factor-alpha regulate different transcriptional and alternative splicing networks in primary beta-cells. *Diabetes* 2010, *59*, 358–374.

[28] Higami, Y., Barger, J. L., Page, G. P., Allison, D. B. et al., Energy restriction lowers the expression of genes linked to inflammation, the cytoskeleton, the extracellular matrix, and angiogenesis in mouse adipose tissue. *J. Nutr.* 2006, *136*, 343–352.

[29] Cancello, R., Henegar, C., Viguerie, N., Taleb, S. et al., Reduction of macrophage infiltration and chemoattractant gene expression changes in white adipose tissue of morbidly obese subjects after surgery-induced weight loss. *Diabetes* 2005, *54*, 2277–2286.

[30] Morton, N. M., Nelson, Y. B., Michailidou, Z., Di Rollo, E. M. et al., A stratified transcriptomics analysis of polygenic fat and lean mouse adipose tissues identifies novel candidate obesity genes. *PLoS One* 2011, *6*, e23944.

[31] Koza, R. A., Nikonova, L., Hogan, J., Rim, J. S. et al., Changes in gene expression foreshadow diet-induced obesity in genetically identical mice. *PLoS Genet.* 2006, *2*, e81.

[32] Tobias, P. S., Soldau, K., Ulevitch, R. J., Identification of a lipid A binding site in the acute phase reactant lipopolysaccharide binding protein. *J. Biol. Chem.* 1989, *264*, 10867–10871.

[33] Battafaraono, R. J., Dahlberg, P. S., Ratz, C. A., Johnston, J. W. et al., Peptide derivatives of three distinct lipopolysaccharide binding proteins inhibit lipopolysaccharide-induced tumor necrosis factor-alpha secretion in vitro. *Surgery* 1995, *118*, 318–324.

[34] Su, G. L., Freeswick, P. D., Geller, D. A., Wang, Q. et al., Molecular cloning, characterization, and tissue distribution of rat lipopolysaccharide binding protein. Evidence for extrahepatic expression. *J. Immunol.* 1994, *153*, 743–752.

[35] Le, K. A., Mahurkar, S., Alderete, T. L., Hasson, R. E. et al., Subcutaneous adipose tissue macrophage infiltration is associated with hepatic and visceral fat deposition, hyperinsulinemia, and stimulation of NF-kappaB stress pathway. *Diabetes* 2011, *60*, 2802–2809.

[36] Park, B. S., Song, D. H., Kim, H. M., Choi, B. S. et al., The structural basis of lipopolysaccharide recognition by the TLR4-MD-2 complex. *Nature* 2009, *458*, 1191–1195.

[37] Shi, H., Kokoeva, M. V., Inouye, K., Tzameli, I. et al., TLR4 links innate immunity and fatty acid-induced insulin resistance. *J. Clin. Invest.* 2006, *116*, 3015–3025.

[38] He, G. Z., Zhou, K. G., Zhang, R., Chen, X. F., The effects of n-3 PUFA and intestinal lymph drainage on high-mobility group box 1 and Toll-like receptor 4 mRNA in rats with intestinal ischaemia-reperfusion injury. *Br. J. Nutr.* 2011, DOI: 10.1017/S0007114511006040.

[39] Youn, J. H., Kwak, M. S., Wu, J., Kim, E. S. et al., Identification of lipopolysaccharide-binding peptide regions within HMGB1 and their effects on subclinical endotoxemia in a mouse model. *Eur. J. Immunol.* 2011, *41*, 2753–2762.

[40] Kallio, K. A., Buhlin, K., Jauhiainen, M., Keva, R. et al., Lipopolysaccharide associates with pro-atherogenic lipoproteins in periodontitis patients. *Innate. Immun.* 2008, *14*, 247–253.

[41] Osto, M., Zini, E., Franchini, M., Wolfrum, C. et al., Subacute endotoxemia induces adipose inflammation and changes in lipid and lipoprotein metabolism in cats. *Endocrinology* 2011, *152*, 804–815.

[42] Levine, D. M., Parker, T. S., Donnelly, T. M., Walsh, A. et al., In vivo protection against endotoxin by plasma high density lipoprotein. *Proc. Natl. Acad. Sci. USA* 1993, *90*, 12040–12044.

[43] Jiang, X. C., Bruce, C., Mar, J., Lin, M. et al., Targeted mutation of plasma phospholipid transfer protein gene markedly reduces high-density lipoprotein levels. *J. Clin. Invest.* 1999, *103*, 907–914.

[44] Suzuki, T., Hara, H., Dietary fat and bile juice, but not obesity, are responsible for the increase in small intestinal permeability induced through the suppression of tight junction protein expression in LETO and OLETF rats. *Nutr. Metab. (Lond).* 2010, *7*, 19.

[45] Raimondi, F., Santoro, P., Barone, M. V., Pappacoda, S. et al., Bile acids modulate tight junction structure and barrier function of Caco-2 monolayers via EGFR activation. *Am. J. Physiol. Gastrointest. Liver Physiol.* 2008, *294*, G906–G913.

[46] Houdijk, A. P., Meijer, C., Cuesta, M. A., Meyer, S. et al., Perioperative anti-endotoxin strategies. *Scand. J. Gastroenterol. Suppl.* 1997, *222*, 93–97.

[47] Widberg, C. H., Newell, F. S., Bachmann, A. W., Ramnoruth, S. N. et al., Fibroblast growth factor receptor 1 is a key regulator of early adipogenic events in human preadipocytes. *Am. J. Physiol. Endocrinol. Metab.* 2009, *296*, E121–E131.

[48] Yang, K., Guan, H., Arany, E., Hill, D. J. et al., Neuropeptide Y is produced in visceral adipose tissue and promotes proliferation of adipocyte precursor cells via the Y1 receptor. *FASEB J.* 2008, *22*, 2452–2464.

[49] Catalioto, R. M., Maggi, C. A., Giuliani, S., Chemically distinct HDAC inhibitors prevent adipose conversion of subcutaneous human white preadipocytes at an early stage of the differentiation program. *Exp. Cell. Res.* 2009, *315*, 3267–3280.

[50] Swierczynski, J., Zabrocka, L., Goyke, E., Raczynska, S. et al., Enhanced glycerol 3-phosphate dehydrogenase activity in adipose tissue of obese humans. *Mol. Cell. Biochem.* 2003, *254*, 55–59.

[51] Gesta, S., Bluher, M., Yamamoto, Y., Norris, A. W. et al., Evidence for a role of developmental genes in the origin of obesity and body fat distribution. *Proc. Natl. Acad. Sci. USA* 2006, *103*, 6676–6681.

[52] Marshall, C. B., Krofft, R. D., Blonski, M. J., Kowalewska, J. et al., Role of smooth muscle protein SM22alpha in glomerular epithelial cell injury. *Am. J. Physiol. Renal. Physiol.* 2011, *300*, F1026–F1042.

[53] Cao, Y., Angiogenesis modulates adipogenesis and obesity. *J. Clin. Invest.* 2007, *117*, 2362–2368.

[54] Pendas, A. M., Folgueras, A. R., Llano, E., Caterina, J. et al., Diet-induced obesity and reduced skin cancer susceptibility in matrix metalloproteinase 19-deficient mice. *Mol. Cell. Biol.* 2004, *24*, 5304–5313.

[55] Moya, M. L., Lucas, S., Francis-Sedlak, M., Liu, X. et al., Sustained delivery of FGF-1 increases vascular density in comparison to bolus administration. *Microvasc. Res.* 2009, *78*, 142–147.

[56] Ivanciu, L., Gerard, R. D., Tang, H., Lupu, F. et al., Adenovirus-mediated expression of tissue factor pathway inhibitor-2 inhibits endothelial cell migration and angiogenesis. *Arterioscler. Thromb. Vasc. Biol.* 2007, *27*, 310–316.

[57] Christianson, J. L., Nicoloro, S., Straubhaar, J., Czech, M. P., Stearoyl-CoA desaturase 2 is required for peroxisome proliferator-activated receptor gamma expression and adipogenesis in cultured 3T3-L1 cells. *J. Biol. Chem.* 2008, *283*, 2906–2916.

[58] Warne, J. P., John, C. D., Christian, H. C., Morris, J. F. et al., Gene deletion reveals roles for annexin A1 in the regulation of lipolysis and IL-6 release in epididymal adipose tissue. *Am. J. Physiol. Endocrinol. Metab.* 2006, *291*, E1264–E1273.

[59] Cao, Y., Adipose tissue angiogenesis as a therapeutic target for obesity and metabolic diseases. *Nat. Rev. Drug Discov.* 2010, *9*, 107–115.

[60] Xue, Y., Petrovic, N., Cao, R., Larsson, O. et al., Hypoxia-independent angiogenesis in adipose tissues during cold acclimation. *Cell Metab.* 2009, *9*, 99–109.

[61] Trayhurn, P., Wood, I. S., Adipokines: inflammation and the pleiotropic role of white adipose tissue. *Br. J. Nutr.* 2004, *92*, 347–355.

[62] Pang, C., Gao, Z., Yin, J., Zhang, J. et al., Macrophage infiltration into adipose tissue may promote angiogenesis for adipose tissue remodeling in obesity. *Am. J. Physiol. Endocrinol. Metab.* 2008, *295*, E313–E322.

[63] Miranda, M., Chacon, M. R., Gutierrez, C., Vilarrasa, N. et al., LMNA mRNA expression is altered in human obesity and type 2 diabetes. *Obesity (Silver Spring)* 2008, *16*, 1742–1748.

[64] Pihlajamaki, J., Lerin, C., Itkonen, P., Boes, T. et al., Expression of the splicing factor gene SFRS10 is reduced in human obesity and contributes to enhanced lipogenesis. *Cell Metab.* 2011, *14*, 208–218.

[65] Salati, L. M., Szeszel-Fedorowicz, W., Tao, H., Gibson, M. A. et al., Nutritional regulation of mRNA processing. *J. Nutr.* 2004, *134*, 2437S–2443S.

[66] Sakla, M. S., Lorson, C. L., Induction of full-length survival motor neuron by polyphenol botanical compounds. *Hum. Genet.* 2008, *122*, 635–643.

[67] Fernandez, C. M., Molto, E., Gallardo, N., Del Arco, A. et al., The expression of rat resistin isoforms is differentially regulated in visceral adipose tissues: effects of aging and food restriction. *Metabolism* 2009, *58*, 204–211.

[68] Lin, J. C., Tarn, W. Y., RBM4 down-regulates PTB and antagonizes its activity in muscle cell-specific alternative splicing. *J. Cell Biol.* 2011, *193*, 509–520.

[69] Nathan, D. M., Davidson, M. B., DeFronzo, R. A., Heine, R. J. et al., Impaired fasting glucose and impaired glucose tolerance: implications for care. *Diabetes Care* 2007, *30*, 753–759.

